Phase Separation in Binary Polymer/Liquid Crystal Mixtures: Network Breaking and Domain Growth by Coalescence-induced Coalescence

Iryna Demyanchuk,[†] Stefan A. Wieczorek,*[,†] and Robert Hołyst[†,‡]

Institute of Physical Chemistry, Polish Academy of Sciences, Kasprzaka 44/52, 01-224 Warsaw, Poland, and Department of Mathematics and Natural Sciences, College of Science, Cardinal Stefan Wyszyñski University, Dewajtis 5, 01-815 Warsaw, Poland

Received: December 20, 2005; In Final Form: March 14, 2006

A small-angle light scattering (SALS) technique together with optical microscopy observation are used to investigate phase separation kinetics in films of low molecular weight thermotropic liquid crystal (4-cyano-4′-*n*-octyl-biphenyl, 8CB) with flexible polymer (polystyrene, PS). The growth of domains is studied as a function of time, film thickness, and film composition. The light scattering results are correlated with the images obtained by optical microscopy observation. In this paper, we study the breaking of a bicontinuous network of polymer in liquid crystal into droplets and their further growth via the coalescence-induced coalescence mechanism. The appearance of droplets in the system leads to a strong scattering at small wave vectors, while the bicontinuous network gives a peak at a nonzero wave vector. Superposition of these scattering intensities leads to the appearance of a second peak in the full scattering intensity signal, when the bicontinuous network starts to break up into disjointed elongated domains. Finally, both peaks merge into a single peak, which moves quickly toward zero wave vectors, indicating a complete transformation of elongated domains into spherical droplets of variable size. We found that the separation process does not depend on the size of the system. Irrespective of the sample thickness, the network breaks into fragments always at the same time after temperature quench. On the basis of morphological analysis, we found that the average size of the droplets which formed from the network grows with time, t, as t^{α}, $\alpha = 0.9 \pm 0.1$, in the isotropic phase and in the nematic phase.

1. Introduction

The phase separation/mixing are ubiquitous in polymer technology. Usually, the final industrial products have mechanical, transport, electrical, and so forth, properties which depend on the kinetics and dynamics of the separation/mixing process used in their formation.[1,2] In particular, the product property depends on the final morphology in the system, that is, the shape and sizes of domains obtained in the phase separation. The separation process in a liquid state can be stopped at any stage by rapid vitrification (solidification) of the separating mixture, and the morphology produced at this moment stays inside a solid material determining its final properties. From this technological perspective, it is crucial to understand the morphological transformations during phase separation in liquid mixtures. In general, we can have two different morphological structures inside the binary liquid A/B mixture: bicontinuous and droplet patterns. In the first case, A-rich and B-rich domains are continuous across the system. We call them percolating domains. In the second case of droplet morphology, one of the components, say B, forms B-rich domains in the continuous A-rich matrix. In the process of phase separation, we do expect that there is a ubiquitous morphological bicontinuous-droplet transformation (percolation-to-droplet transition). It can be caused by the volumetric differences between phases or by different wetting properties. A minority phase of volume fraction below the percolation threshold (around 30%) must break into disjoint domains. Similarly, when the A-rich phase completely wets the container walls, the B-rich phase would also break into domains. For binary mixtures, characterized by the asymmetric volume fraction of emerging phases, the percolation-to-droplets (PDT) morphology transition has been observed.[3−5] During this structural transition, the bicontinuous and the droplets morphologies are both present in the system. At the beginning of the separation process in the binary A/B mixture, when the asymmetry in the volume fraction is not too large, two types of domains (A-rich and B-rich) are continuous through the whole sample. The domains grow (coarsen), saturate, and change their volumes. At a certain moment of coarsening, the minority phase cannot maintain volumetrically the macroscopic percolation (continuity) and, as a result, the bicontinuous network breaks up into fragments. To minimize the interfacial free energy, the fragmented network quickly collapses into spherical droplets. The percolation-to-droplet transformation is studied here in a polymer/liquid crystal mixture by light scattering and optical microscopy.

The late stage configuration of the separated mixture does not depend on earlier mechanisms of separation. Only the size of the system, initial volume fractions, and wetting properties influence the late stage growth. There are a few different mechanisms of domain growth in the late stage.[3−11] In the case of the vanishing small volume fraction of the minority phase, the "evaporation−condensation" mechanism of domains growth is observed. This process was first described by Lifshitz, Slyozov, and Wagner (LSW mechanism).[6] Small droplets decrease in size, and the molecules from them diffuse toward

* To whom correspondence should be addressed. E-mail: wieczor@ichf.edu.pl.
† Polish Academy of Sciences.
‡ Cardinal Stefan Wyszyñski University.

10.1021/jp0574091 CCC: $33.50
Published on Web 04/28/2006

large droplets which grow with the growth rate $L(t) \sim t^{1/3}$, where $L(t)$ is the average droplet size and t is time. In the opposite limit of comparable volume fractions of two phases, we usually have a dense system of droplets and, in this case, the process called coalescence-induced coalescence (CIC) occurs.[7−11] There are three different mechanisms of CIC: "coalescence-induced coalescence via flow", "coalescence-induced coalescence via diffusion", and "geometrical coalescence-induced coalescence". The process, when coalescence between two droplets induces the next coalescence, via a hydrodynamic flow induced in the matrix, is called "coalescence-induced coalescence via flow". A few droplets that are close together, exhibiting overlapping concentration fields around them, can merge due to the diffusion of molecules induced by the concentration gradients. The overlapping fields lead also to the long-range attractive interactions between them. This mechanism is the "coalescence-induced coalescence via diffusion". Finally, the process, when two droplets experience a collision, change their shape, and in the process, touch another droplet and induce a second coalescence, is called the "geometrical coalescence-induced coalescence". Through the use of computer simulations, it was predicted[10] that the growth rate for the coalescence-induced coalescence via diffusion $L(t) \sim t^{1/3}$ and $L(t) \sim t$ for the coalescence-induced coalescence via flow. Interestingly, the CIC mechanism seems to be universal, not dependent upon the material properties of a particular mixture. It has been observed so far in poly(vinyl methyl)ether and water;[10] ϵ-caprolactone oligomer and styrene oligomer;[10] *n*-dodecyl hexaoxyethylene glycol monoether and water;[12] *n*-dodecyl hexaoxyethylene glycol monoether, water, and poly(ethylene glycol);[12] poly(methylphenylsiloxane) and polystyrene mixture;[5] isotactic polypropylene and diphenyl ether.[13] Here, we show that the same mechanism of growth occurs in the binary polymer/liquid crystal mixture (8CB/PS (4-cyano-4′-*n*-octyl-biphenyl/polystyrene). Moreover, for the first time, we show that the coalescence-induced coalescence mechanism also occurs in the ordered liquid crystalline matrix and thus is not restricted to the isotropic liquids. Moreover, we determine experimentally the exponent of growth for the CIC in ordered and disordered matrixes (i.e., isotropic and nematic).

Homogeneous mixtures consisting of liquid crystals and polymers are widely used for display applications, gas flow sensors, optical gratings, memories, infrared shutters, optical sensors, and so forth.[14] The applications make the liquid crystal/polymer binary mixtures and their phase separation an important object of research. Here, we study the phase separation process in the mixture of 8CB/PS (4-cyano-4′-*n*-octyl-biphenyl/polystyrene). The changes in morphology of the separated system are detected by light scattering and optical microscopy. The phase separation process is studied for different concentrations of 8CB in the isotropic or ordered nematic phase.

Light scattering (LS) experiments[15−29] and the direct microscopy observation (MO)[3−5,12,30] are two popular techniques for studying phase separation. Their combination allows us to observe the separation process in the extended time and length scales, since the LS technique gives good results for domain sizes between 0.5 and 5 μm whereas the OM can be used for domains larger than a few micrometers up to sizes exceeding hundreds of micrometers. We have recently[5] combined these two techniques and showed how on the basis of LS we can determine the moment of percolation-to-droplet transition. Here, we will also correlate LS data and OM images to observe this transition. We will show that in the system of percolating domains the growth, $L(t) \sim t^{\alpha}$, is governed by diffusion of components leading to the characteristic exponent of growth $\alpha = {}^1/_3$. After the morphological percolation-to-droplet transition, the mechanism of growth changes to geometrical and CIC induced by flows which are characterized by $\alpha = 1$. We will also mention the influence of the wetting on the separation process.

The questions posed in the manuscript are as follows. How does the late stage phase separation in the 8CB/PS mixture proceed? Does the process depend on the sample thickness? What is the dominating mechanism of growth in the late stage of separation when the domain sizes become comparable to the sample thickness? How does the growth process depend on the ordering in the liquid crystal?

2. Experimental Section

2.1. Sample Preparation and Characterization. Our binary mixture consists of polystyrene (PS) from Fluka Chemical Co. ($M_w = 74\,500$, $M_w/M_n = 1.03$) and a liquid crystal 4-cyano-4′-*n*-octyl-biphenyl (8CB) from the Military University of Technology, Warsaw, Poland. We observe that pure 8CB is an isotropic liquid for temperatures above $T_1 = 40.8 \pm 0.05$ °C, smectic-A below $T_2 = 33.8 \pm 0.05$ °C, and nematic for $T_1 > T > T_2$. In the isotropic phase, the refractive index of 8CB is $n_{8CB} = 1.566$. The refractive index of PS is $n_{PS} = 1.589$, so, we have $\Delta_n = 0.023$. This small difference in the refractive indexes guarantees that in the light scattering experiments in the isotropic phase we do not have multiple scattering of light.

We prepared thin films of different thicknesses for microscopic and light scattering experiments using the following procedure. The mixtures of 8CB/PS at compositions 60/40, 75/25, and 90/10 wt % were dissolved in toluene and then stirred mechanically for 20 h. Films, 10 and 100 μm thick, were prepared by casting from 20% of toluene solutions onto circular glass plates, 0.15 mm thick × 10 mm diameter, cut from microscope cover glass. The uncovered films were dried and annealed for 36 to 48 h at a temperature of 70 °C, just above the cloud point temperature. Next, the film was covered with a second glass plate. The distance between the glasses plates was set by metal spacers of known thickness, 10 or 100 μm, placed between the plates.

2.2. Light Scattering and Optical Microscopy. The changes of the morphology in the mixture of 8CB/PS were studied by the elastic LS experiments using the $\lambda = 632.8$ μm wavelength radiation from a standard He−Ne (5 mW) laser. The light scattering intensity was recorded on a linear array of 512 photodiodes for the scattering angles between $\theta = 0.5°-25°$ corresponding to the wave vectors $q = 0.2-6.9$ μm^{-1}. The values of scattered light intensity I, time t, and temperature T were simultaneously registered at every 0.5 s at the beginning of experiment, and with a lapse of time, this interval time was adjusted between 5 and 30 s depending on how fast the process was going. The final results are shown with the data averaged over 10 nearest photodiodes by the moving average method. The samples of different thicknesses $h = 10$ and 100 μm were used in LS experiments.

For microscopic observation, we used the optical polarizing microscope Nikon ECLIPSE E 400 equipped with Nikon Digital Camera DXM 1200 and a heating/cooling stage LINKAM THMS 600 with 0.01° control of the temperature. The samples of thickness $h = 10$ μm were observed for 24 h, with intervals of 10 min. The photographs during experiments were taken under the magnification of 750X. We used the image analyzing program LUCIA to study the observed image quantitatively.

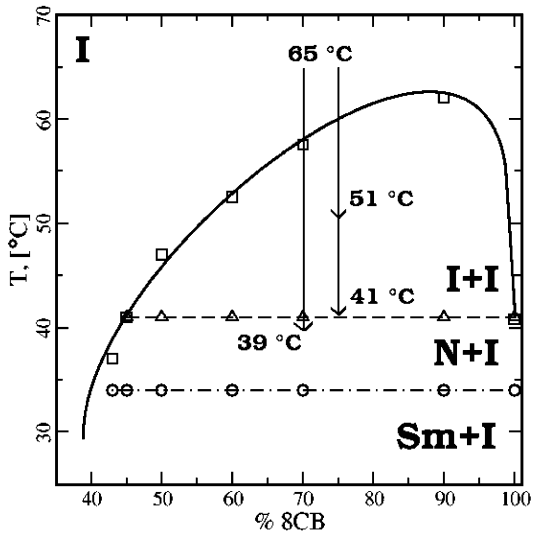

Figure 1. Equilibrium phase diagram of 8CB/PS ($M_w = 74\,500$ g/mol) obtained by optical microscopy (temperature vs concentration of 8CB). The transition temperature from isotropic 8CB + isotropic PS (I + I) to homogeneous, isotropic mixture (I) is represented by squares. The transition temperature from nematic 8CB + isotropic PS (N + I) to isotropic 8CB + isotropic PS (I + I) is shown by triangles. The circles represent the transition temperature from smectic 8CB + isotropic PS (Sm + I) to nematic 8CB + isotropic PS (N + I) regions. Separation is studied at three different temperatures, 39, 41, and 51 °C, and for three different compositions, 90/10, 75/25, and 60/40. Solid lines are guides to the eyes only.

3. Results and Discussion

3.1. Equilibrium Phase Diagram Determination. The phase diagram 8CB/PS shown in Figure 1 has been obtained by the thermomicroscopy studies on an optical polarizing microscope Nikon ECLIPSE E 400, equipped with Nikon Digital Camera DXM 1200 and a heating/cooling stage LINKAM THMS 600. The measurements were performed for seven compositions of 8CB/PS: 46/54, 50/50, 60/40, 70/30, 75/25, and 90/10 wt %, and for pure 8CB. The measurements start at a temperature above phase separation (70 °C) in the homogeneous isotropic phase of the binary mixture. The (I + I) region of the phase diagram was identified on the basis of the cloud point measurements using LS and OM. The liquid crystalline ordered phases, nematic and smectic, were identified on the basis of textures obtained under crossed polarizers. The phase diagram exhibits an upper critical solution temperature and shows four different regions, depending on the ordering of liquid crystal/polymer (the liquid crystal can form in a separating mixture isotropic I, nematic N, and smectic Sm phases, and the polymer can only form an isotropic I phase). We find an isotropic (I) region on the phase diagram, where both components mix; isotropic + isotropic (I + I), where they separate into two isotropic phases; nematic + isotropic (N + I), where the LC-rich phase is in the nematic state; and a smectic + isotropic (Sm + I) region, where the LC-rich phase is in the smectic state. The phase diagram exhibits a large (I + I) miscibility gap which is characteristic for the large molecular weight of PS. For a small molecular weight (of the order of 10 000), the (I + I) region disappears. The transition temperatures to the nematic (N + I) region and smectic (Sm + I) region phases of the liquid crystal do not depend on the composition of the mixture within the experimental error of 0.2°. Thus, the temperature ranges of (N + I) and (Sm + I) regions are set by the isotropic-to-nematic and nematic-to-smectic transition temperatures in pure liquid crystal, respectively.

3.2. Light Scattering Measurements and Optical Microscopy Observations. Light scattering (LS) and optical microscopy (OM) were used to study the kinetics of phase separation in the 8CB/PS mixture. These two methods are complementary. LS gives the morphology changes even when the domain size was smaller than 1 μm. Such small domains were barely observable under OM. On the other hand, when the domain size is bigger than 5−7 μm, the signal obtained in LS is outside the photodiodes array but could easily be studied by the OM method. Thus, LS and OM are two complementary methods for studying phase separation. LS and OM together allow the study of domains of size of the order of 0.5 μm up to 100 μm.

The samples of thickness $h = 10$ and 100 μm are used for LS measurements and $h = 10$ μm for OM observations. The samples are cooled from isotropic phase region (I) to isotropic 8CB + isotropic PS (I + I) and to nematic 8CB + isotropic PS (N + I) phase regions on the equilibrium phase diagram (Figure 1). In the LS experiments, we checked the phase separation process only in the (I + I) phase region. In the (N + I) region, multiple scattering coming from the large difference in ordinary and extraordinary refractive indexes of liquid crystals precluded LS measurements. In the LS measurements, the dominating wave−vector component (q_{max}) gives the maximum of scattering intensity ($I(q,t)$) and is inversely proportional to the size of the domains $L(t) \sim 1/q_{max}(t)$ in the case of bicontinuous, percolating domains. In the optical microscopy measurements, the domain size is observed directly under the microscope.

Figure 2 presents the time evolution of the LS intensity $I(q,t)$ for the 8CB/PS for three compositions: (a) 75/25 wt %, (b) 60/40 wt %, with both mixtures cooled from 65 to 41 °C in the (I + I) region, and (c) 90/10 wt % cooled from 65 to 51 °C in the (I + I) region. Figure 3 shows the OM observation of the phase separation in the mixture of 8CB/PS 75/25 wt % that is cooled from 65 to 41 °C in the (I + I) region. At the beginning of the separation process only the bicontinuous network is observed, Figure 3a (20 min), then the network coarsens and small droplets appear in the system, Figure 3b (40 min). The droplets lead to the increase in the scattering intensity at zero wave vectors. Finally, a bicontinuous network starts to break and the elongated domains appear in the system which later transforms into the spherical droplets minimizing the free interfacial energy, Figure 3c (150 min). Interestingly (ref 5), breaking of the network shows up in the LS measurements (Figure 2) by the appearance of two peaks (one coming from the dense system of droplets and one from the bicontinuous network). Very quickly both peaks merge into one peak, which quickly shifts into zero wave vectors.

When comparing LS spectra (Figure 2) with direct MO (Figure 3) for the same mixtures with $h = 10$ μm, we note that when a bicontinuous network is observed in the sample (Figure 3a), only one peak (peak 1) is detected by LS measurements. A bicontinuous network and small droplets ($\langle D \rangle \ll h$) are presented in the sample together (Figure 3b) for longer times, and as a result, in the LS spectra, there is a signal at the zero wave vectors (coming from polydisperse small droplets[5]). The second peak (peak 2) corresponds to the large domains appearing in the system (Figure 3c) coming from the network which breaks. It is known that when the growth of the first peak in the LS (corresponding to the bicontinuous network) becomes very slow (essentially pinned down) the breaking process of the bicontinuous structure starts. The full process is called the percolation-to-droplets (PDT) morphology transition. As it is shown, PDT starts at the very beginning of the phase separation in 8CB/PS mixture. The growth of the scattering intensity at

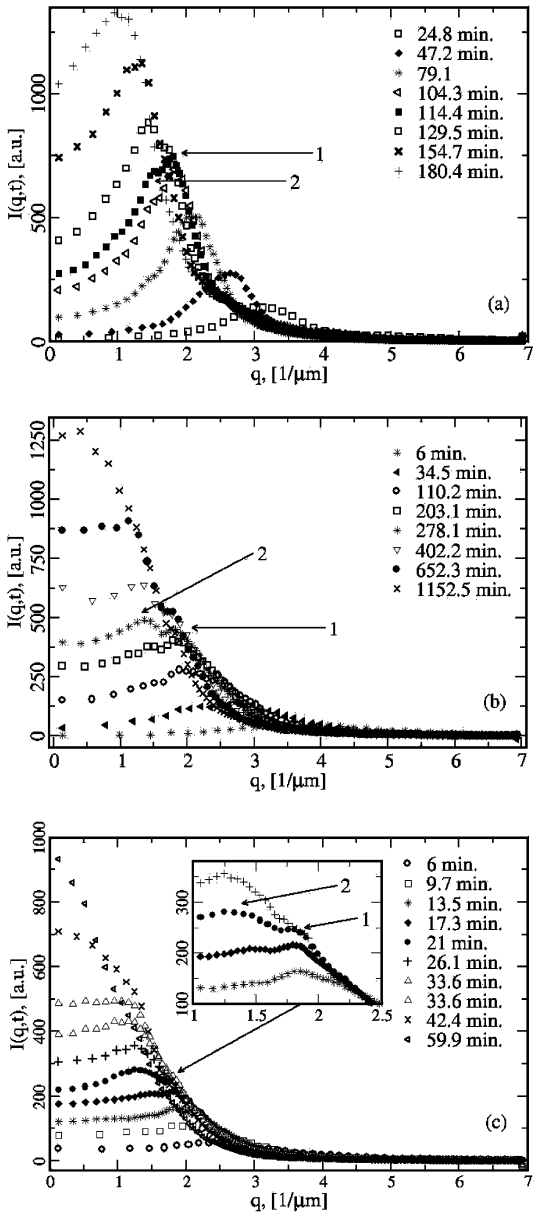

Figure 2. Time evolution of the LS intensity $I(q,t)$ obtained for 8CB/PS: (a) 75/25 wt %, (b) 60/40 wt %, and (c) 90/10 wt %. Mixtures a and b were cooled from 65 °C to 41 °C in the (I + I) region, and sample c was cooled from 65 to 51 °C in the (I + I) region; all of the samples had a thickness of $h = 10$ μm. Peak 1 corresponds to the bicontinuous network present in the system. The peak shifts toward smaller wave vectors indicating the coarsening of the network, which eventually breaks into elongated domains when the growth of the first peak stops. Peak 2 corresponds to the large droplets. The scattering intensity at small wave vectors corresponds to the polydisperse system of small droplets.[5]

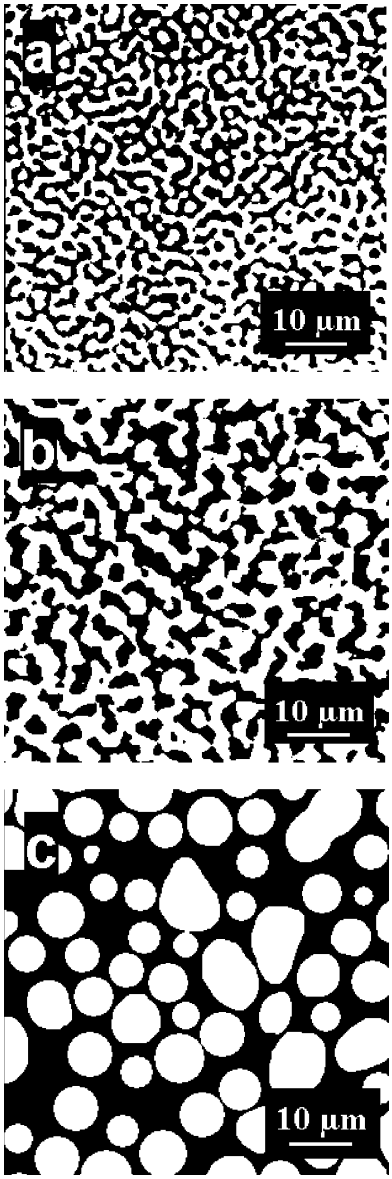

Figure 3. Optical microscopy observation of the phase separation in the mixture of 8CB/PS 75/25 wt % that was cooled from 65 to 41 °C in the (I + I) region, polymer-rich phase (white), and LC-rich phase (black). At the beginning of the separation process only the bicontinuous network is observed (a) (20 min), then the network coarsens and small droplets appear in the system (b) (40 min). The bicontinuous network breaks and the elongated domains appear and transform to the spherical droplets minimizing the free interfacial energy (c) (150 min).

zero q vectors and a single peak at nonzero q vectors are clear indicators that there are small droplets and a bicontinuous network together in the system.

We have used LS measurements to see if the growth of the domains and the moment of PDT depends on the system size and checked the LS signal for thicknesses $h = 10$ μm and $h = 100$ μm. Figure 4 shows the double logarithmic plot of the time evolution of $q_{max}(t)$ for the network peak (Figure 2 (peak 1)) in the 8CB/PS 75/25 wt % mixture cooled from 65 to 41 °C (a, b) and to 51 °C (c, d) in the (I + I) region, for the samples of thicknesses (a, c) $h = 10$ μm and (b, d) $h = 100$ μm. By correlating the results obtained for the samples of different thicknesses, we note that the first peak stops shifting toward the smaller q vectors (bicontinuous network breaks) at the same time for the samples under the same temperature regimes. For the 8CB/PS 75/25 wt % mixture cooled from 65 to 41 °C (a, b), we note that the PDT process starts at $t \approx 140$ min and, for the higher temperature regime (51 °C), it starts at $t \approx 13$ min. For all samples, the growth rule for the first peak is $q(t) \sim t^{-1/3}$, that is, $L(t) \sim 1/q(t) \sim t^{1/3}$ irrespective of the sample thickness. Thus, the moment when the network breaks into elongated domains (PDT transition starts) and the mechanism of the growth do not depend on the sample size.

When the domains sizes are comparable to the size of the system ($\langle D \rangle > \cong 5-7$ μm), the signal obtained in LS measurements gets out of the photodiodes array. To find which mechanism of growth dominates in the sample at late time, we used the OM method. The binary images were obtained and

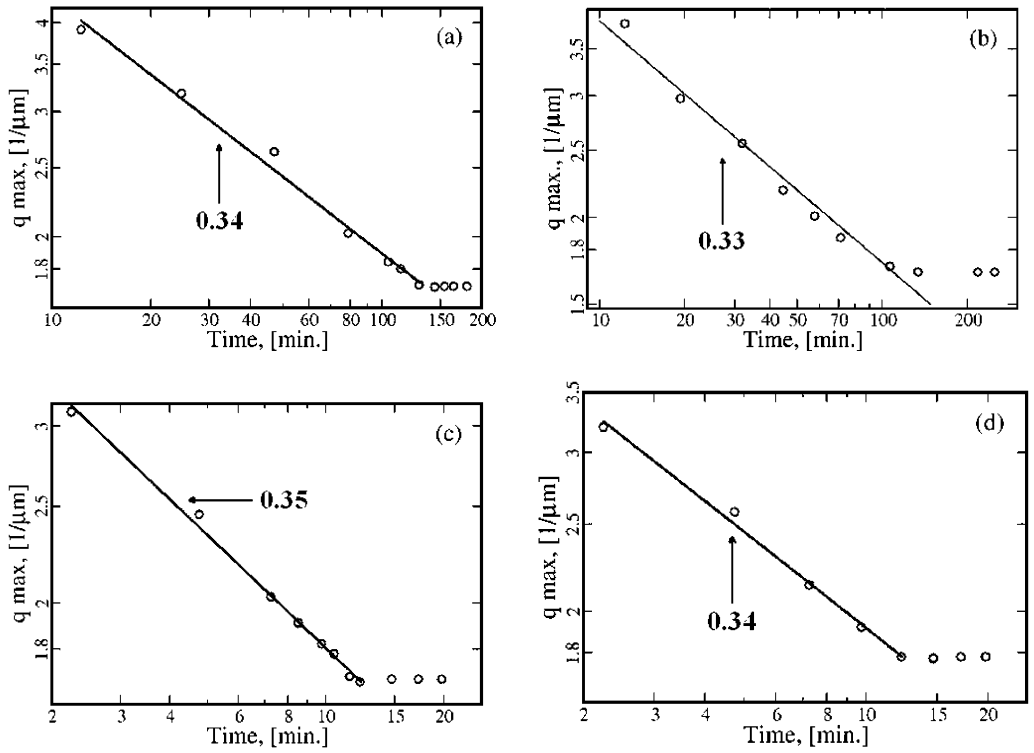

Figure 4. Double logarithmic plot of the time evolution of $q_{max}(t)$ for peak 1 (Figure 2) in the 8CB/PS 75/25 wt % mixture cooled from 65 to 41 °C (a, b) and to 51 °C (c, d) in the (I + I) region, for the samples of thickness (a, c) $h = 10$ μm and (b, d) $h = 100$ μm. The growth rule for the first peak is $q(t) \sim t^{-1/3}$ (domain size $L(t) \sim 1/q(t) \sim t^{1/3}$) irrespective of the sample thickness (a, b, c, and d). Thus, the separation process does not depend on the size of the system. The moment when the network breaks into fragment does not depend on the sample size as well ((a, b) and (c, d)). (In the Supporting Information, graphs of $q_{max}(t)$ for the compositions 60/40 wt % and 90/10 wt % are shown.)

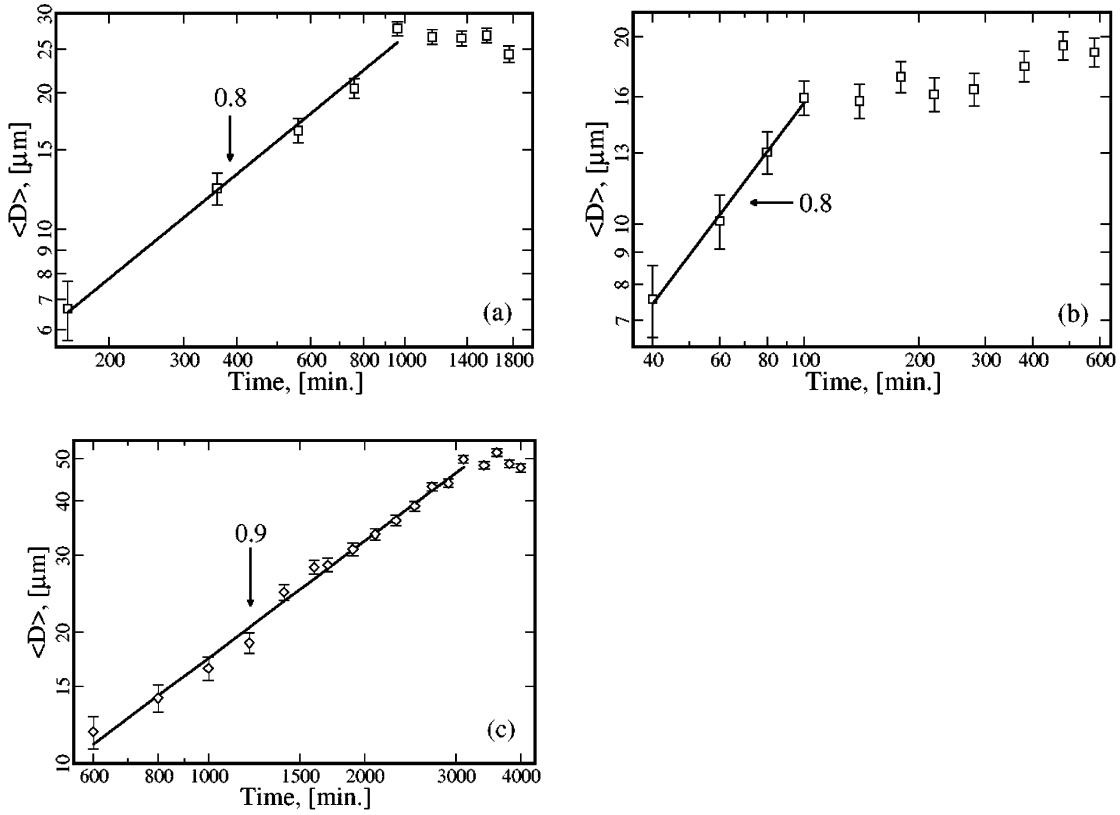

Figure 5. Time evolution of the mean domains diameter $\langle D \rangle$ for the 8CB/PS 75/25 wt % mixture that was cooled from 65 °C to (a) 41 °C in the (I + I) region, (b) 51 °C in the (I + I) region, and (c) 39 °C in the (N + I) region. In all microscopic observations, the thickness of the films was equal to 10 μm. The droplets grow as $t^{0.8-0.9}$ via the geometrical coalescence-induced coalescence mechanism (Figure 6). The same growth rate is observed in the isotropic 8CB + isotropic PS (I + I) and in the nematic 8CB + isotropic PS (N + I) phase regions of the equilibrium phase diagram (a, b, and c). (In the Supporting Information, a graph of $\langle D \rangle$ vs time for 90/10 wt % is shown.)

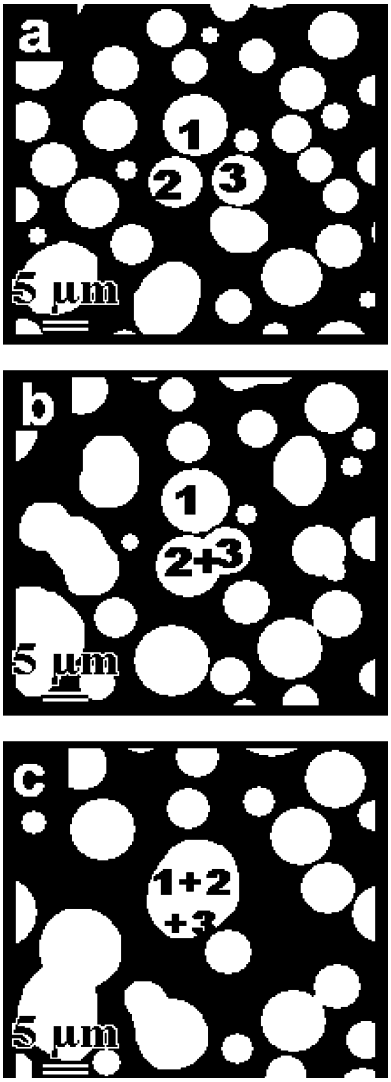

Figure 6. Geometrical coalescence-induced coalescence in the mixture of 8CB/PS 75/25 wt % cooled from 65 to 51 °C in the (I + I) region after (a) 40 min, (b) 50 min, and (c) 60 min. The white color represents the polymer-rich domains, and the black color represents the LC-rich phase. The coalescence between domains 1 and 2 (a) induces the change of shape of the resulting domain 1 + 2 (b), which induces coalescence with droplet 3 (c). Please note that a change in geometry will also induce flow around the domain.

analyzed quantitatively. Figure 5 shows the time evolution of the mean domains diameter ($\langle D \rangle$) during the phase separation in the mixture of 8CB/PS 75/25 wt %, which was cooled from 65 °C to (a) 41 °C in the (I + I) region, (b) 51 °C in the (I + I) region, and (c) 39 °C in the (N + I) region. The domains growth was found as $L(t) \sim t^{0.8-0.9}$. The same exponent was found for the samples cooled into the (I + I) and into the (N + I) regions. However, it should be noted that the estimated error connected with extracting exponent α from time evolution of the mean domains diameter $\langle D \rangle$ is of the order ±0.1. The analysis of images showed that the dominating mechanism of growth was CIC. Figure 6 shows geometrical CIC in the mixture of 8CB/PS 75/25 wt % cooled from 65 to 51 °C in the (I + I) region, after (a) 40 min, (b) 50 min, and (c) 60 min. The coalescence between domains 1 and 2 (a) induces the change of shape of the resulting domain 1 + 2 (b), which induces coalescence with droplet 3 (c).

In the very late stage of decomposition, the sizes of domains become much bigger than the system size ($\langle D \rangle \gg 10\ \mu$m). It is interesting that in this regime there is a very strong influence

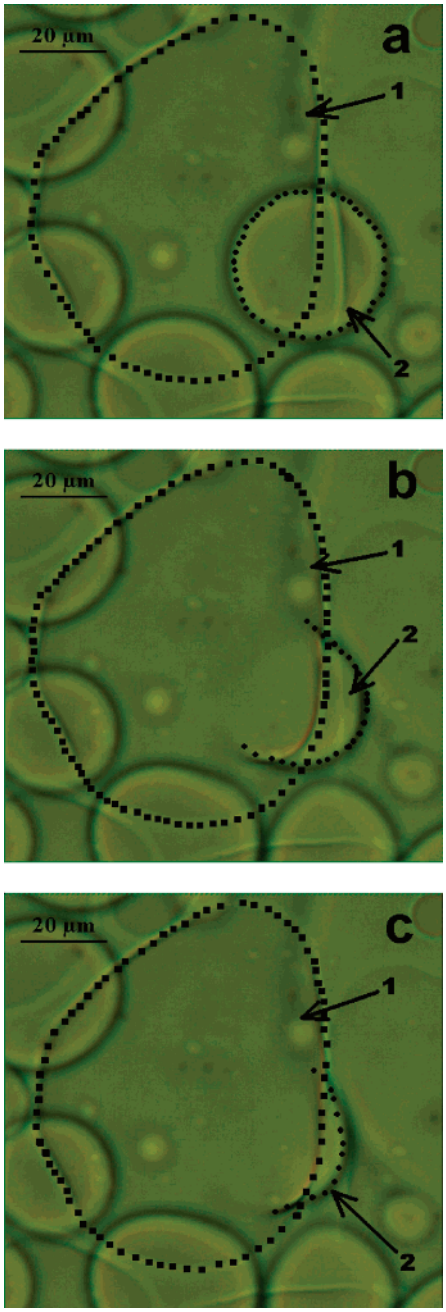

Figure 7. Coalescence of the smaller domain with the huge domain, which wet the glass in the 8CB/PS 75/25 wt % mixture cooled from 65 to 41 °C after (a) 1581 min, (b) 1630 min, and (c) 1690 min. In this case, a droplet bigger than the system size ($\langle D \rangle \gg 10\ \mu$m) touches a huge droplet ($\langle D \rangle \geq 100\mu$m), which wet the glass. Wetting precludes the dimensional crossover (see also a movie in the Supporting Information).

of the wetting behavior on the growth mechanism. Figure 7 shows how the large domains which were spread on the surface "merged" with smaller domains in the bulk. The photographs in Figure 7 are obtained for the 8CB/PS 75/25 wt % mixture cooled from 65 to 41 °C after (a) 1581 min, (b) 1630 min, and (c) 1690 min. Huge domains ($\langle D \rangle \geq 100\ \mu$m) wet the glass surface (a). They are so large that practically we do not see them under the microscope, that is, we do not see their boundaries. However, whenever a smaller domain (of larger curvature) touches the domain which wets the glass, it disappears. The wetting domain sucks the smaller one quickly because of the differences in curvatures and thus of osmotic pressures. The larger osmotic pressure appears in the domain

of larger curvature, and thus, when such a domain touches the large one, the flow of material goes from the smaller to the larger domain. Interestingly, the preferential wetting of the glass by liquid crystal precludes the dimensional crossover observed previously[12] for the surfactant/water mixtures. In this work, we carefully analyzed the morphology evolution during the phase separation process in the binary liquid crystal/polymer mixture (8CB/PS (4-cyano-4′-*n*-octyl-biphenyl/polystyrene)) by both light scattering (LS) and optical microscopy (OM) methods. In the movie in the Supporting Information, we present all stages of morphological changes during phase separation in our system. At first we observe a bicontinuous morphology which coarsens via diffusion. During growth, small droplets appear as a result of local breakage of the network. When the network breaks, the further growth is governed by the coalescence-induced coalescence mechanism. At the later stage, when the domains are much bigger than the size of the system ($\langle D\rangle \gg 10$ μm), the wetting mechanism dominates the growth. In the latter stage, the large domains covering the glass plates "eat" the smaller domains. The geometrical CIC and wetting mechanism of growth are clearly visible in the movie in the Supporting Information.

4. Conclusions

The phase separation process in the binary mixture of 8CB/PS (4-cyano-4′-*n*-octyl-biphenyl/polystyrene) has been studied by both light scattering (LS) and optical microscopy (OM). We have observed that the percolation-to-droplets transition (PDT) starts at the very beginning of the separation process. A growth of scattering at zero wave vectors is a clear indication of this process. Thus, in the sample, we have a bicontinuous network and small droplets. The main scattering peak stops to grow at a certain moment of separation, and we observed under the OM that this moment corresponds to the breakage of the network into large fragments. In the previous work, this behavior and an appearance of the second peak was mistakenly interpreted as a change of growth mechanism from diffusion to hydrodynamic flow.[20] It was found that the separation process does not depend on the size of the system. The growth rule for the first peak is $q(t) \sim t^{-1/3}$ ($L(t) \sim 1/q(t)$) irrespective of the sample thickness, which was varied by an order of magnitude ($h = 10$, 100 μm). The moment when the network breaks into fragments does not depend on the sample size either. Direct OM observation shows that the droplets formed from the network grow as $t^{0.9\pm0.1}$ via the geometrical and flow coalescence-induced coalescence mechanism. The same growth rate was observed in the isotropic 8CB + isotropic PS (I + I) and in the nematic 8CB + isotropic PS (N + I) phase regions of the equilibrium phase diagram.

We note that the sample boundaries influence the growth of the droplets when they are much bigger than the system size. Previously[12] (in the water/surfactant mixture), we have observed a dimensional crossover from the growth characterized by $\alpha = 1$ to $\alpha = {}^1/_3$. The change of the growth exponent was interpreted as the change of the dimensionality of the system (from a 3D to 2D system). Here, we do not observe this behavior because one of the phases wets the wall and in fact precludes the crossover. As a result, huge domains ($\langle D\rangle \geq 100$ μm) which wet the glass surface "eat" smaller domains from the bulk. The movie in the Supporting Information illustrates this point.

Acknowledgment. This work was supported by the KBN Grant No. 3T09A09727 (2004−2007).

Supporting Information Available: Double logarithmic plot of the time evolution of $q_{max}(t)$ for peak 1 in 8CB/PS at various compositions and the time evolution of mean domains diameter $\langle D\rangle$ for the 8CB/PS 90/10 wt % mixture. Movie presenting all stages of morphological changes during phase separation in our system. This material is available free of charge via the Internet at http://pubs.acs.org.

References and Notes

(1) Sperling, L. H. *Introduction to Physical Polymer Science*, 3rd ed.; John Wiley & Sons Inc.: New York, 2001.
(2) Stroble, G. *The physics of polymers*; Springer: Berlin, 1996.
(3) Läuger, J.; Lay, R.; Gronski, W. *J. Chem. Phys.* **1994**, *101*, 7181.
(4) Cabral, J. T.; Higgins, J. S.; Yerina, M. A.; Magonov, S. N. *Macromolecules* **2002**, *35*, 1941.
(5) Demyanchuk, I.; Wieczorek, S. A.; Hołyst, R. *J. Chem. Phys.* **2004**, *121*, 1141.
(6) Bray, A. J. *Adv. Phys.* **1994**, *43*, 357.
(7) Beysens, D. A. *Physica A* **1997**, *239*, 329.
(8) Tanaka, H. *Phys. Rev. Lett.* **1994**, *72*, 1702.
(9) Nikolaev, V. S.; Beysens, D.; Guenoum, P. *Phys. Rev. Lett.* **1996**, *76*, 3144.
(10) Tanaka, H. *J. Chem. Phys.* **1996**, *105*, 10099.
(11) Tanaka, H. *J. Chem. Phys.* **1997**, *107*, 3734.
(12) Demyanchuk, I.; Staniszewski, K.; Hołyst, R. *J. Phys. Chem. B* **2005**, *109*, 4419.
(13) Martula, D. S.; Bonnecaze, R. T.; Lloyd, D. R. *Int. J. Multiphase Flow* **2003**, *29*, 1265−1282. Martula, D. S.; Hasegawa, T.; Lloyd, D. R.; Bonnecaze, R. T. *J. Colloid Interface Sci.* **2000**, *232*, 241.
(14) Kitzerow, H. S. *Liq. Cryst.* **1994**, *16*, 1.
(15) White, W. R.; Wiltzius, P. *Phys. Rev. Lett.* **1995**, *75*, 3012.
(16) Takeno, H.; Nakamura, E.; Hashimoto, T. *J. Chem. Phys.* **1999**, *110*, 7.
(17) Tanaka, H. *J. Phys.: Condens. Matter* **2000**, *12*, R207.
(18) Tanaka, H.; Nakanishi, E.; Takubo, N. *Phys. Rev. E* **2002**, *65*, 021802.
(19) Graca, M.; Wieczorek, S. A.; Fialkowski, M.; Hołyst, R. *Macromolecules* **2002**, *35*, 9117.
(20) Graca, M.; Wieczorek, S. A.; Hołyst, R. *Macromolecules* **2003**, *36*, 6903.
(21) Binder, K.; Stauffer, D. *Phys. Rev. Lett.* **1974**, *33*, 1006.
(22) Binder, K. *Phys. Rev. B* **1977**, *15*, 4425.
(23) Siggia, E. D. *Phys. Rev. A* **1979**, *20*, 595.
(24) Hashimoto, T.; Itakura, M.; Hasegawa, H. *J. Chem. Phys.* **1986**, *85*, 6118.
(25) Komura, S. *Phase Transitions* **1988**, *12*, 3.
(26) Hashimoto, T. *Phase Transitions* **1988**, *12*, 47.
(27) Bates, F. S.; Wiltzius, P. *J. Chem. Phys.* **1989**, *91*, 3258.
(28) Tanaka, H. *Phys. Rev. Lett.* **1993**, *71*, 3158.
(29) Takeno, H.; Hashimoto, T. *J. Chem. Phys.* **1997**, *107*, 1634.
(30) Takeno, H.; Iwata, M.; Tkenaka, M.; Hashimoto, T. *Macromolecules* **2000**, *33*, 9657.